Definition of a single axis excitation set-up for a multi-axial random fatigue assessments

Luca Campello [1,2]*, Raffalla Sesana*[1]*, Vivien Denis* [2]*, Cristiana Delprete*[1]*, Roger Serra*[2]

[1] DIMEAS, Politecnico di Torino, Italy

[2] LaMé, INSA Centre-Val de Loire, France

ABSTRACT

Experimental vibration tests for structural durability assessment are one of the most important steps to estimate the fatigue life of mechanical components. Tests set-up where the components endure uni-axial random loading state may be easier to execute than bi-axial or multi-axial tests. The uni-axial stress can be achieved, for instance, with a cantilever beam mounted onto a shaker producing a bending random loading. On the contrary, a multi-axial stress assessment may require one or more machines, specific testing layout and particular shape of specimen that allow the activation of different loads in different direction at the same time, which may be a tedious task in practice. To mitigate these difficulties, a number of testing methodologies that differ in terms of testing machines, specimen geometry and type of excitation, were proposed in the literature. This paper aims to present a new testing set-up to apply random bending-torsion loading in vibratory test by a uni-directional exciters. The system is composed by a specimen, with rectangular section, mounted onto an electrodynamic shaker and a T-mass shaped placed on the specimen's tip. The eccentricity of the T-mass shaped induces a torsion loading, combined with bending, on the specimen in a specific range of frequency. A finite element model is first used to conduct a design phase analysis to define a suitable dimension of the T-mass shaped, and then to estimate the system dynamic response and the stress distribution on the notched specimen section. The model is calibrated and validated through harmonic tests. From numerical and experimental tests, by means of evaluating the numerical stress components and accelerometers phases, it is shown that the specimen is subjected to a bending-torsion coupled loading if the second mode is excited, and to a pure bending loading when the first, third, and fourth modes are excited. After a numerical validation of the loading cases, fatigue tests with random loading are executed and the experimental results are compared with those obtained with the numerical methods.

Keywords: Dynamic responses; Fatigue life estimation; Multi-axial stress; Random vibration fatigue

1. INTRODUCTION

Throughout their operational lifecycle, mechanical components in various industries are frequently subjected to random vibrational loading, which can lead to progressive fatigue damage and eventual failure. One of the most effective methods for assessing the durability of structures under vibrational loading is through experimental vibration testing. In traditional fatigue testing, multi-axial loading conditions are typically replicated using a uni-axial testing set-up, as these systems are easier to design and implement [1]. However, researchers have shown that uni-axial tests may not fully capture the complex dynamics of multi-axial excitation environments. Specifically, the specimen's response to loading can vary significantly when subjected to multi-directional forces, as opposed to the simpler uni-directional loading typically employed in these tests. This discrepancy arises because the interaction of different loading axes can lead to different stress distributions, deformation modes, and potential failure mechanisms that are not adequately represented in uni-axial testing conditions. As such, relying solely on uni-axial excitation may result in inaccurate predictions of the component's fatigue life, often leading to overly conservative or misleading estimates of failure times [2]. In response to these limitations, numerous researchers have proposed alternative solutions aimed at more accurately simulating multi-axial loading conditions. These solutions vary in complexity and approach, often involving modifications to the geometry of the specimen or the design of the testing equipment [3]. These studies underline the need for testing setups that better replicate the real-world conditions that components experience during their operational life. Inspired by the work of [4] [5], this paper proposes a novel testing set-up designed to allow a sheet to experience torsional deformation. The system is based on a uni-directional shaker, with one extremity of the specimen fixed at its top. A T-mass shaped is attached to the other extremity of the specimen, introducing torsional forces. This configuration is intended to overcome the limitations of simpler testing setups by enabling the specimen to undergo torsional deformation, which is crucial for understanding the fatigue behaviour under more complex loading scenarios. The main objective of this paper is to provide a detailed description of the proposed testing setup, followed by an exploration of the results obtained from a numerical finite element (FE) model that simulates the specimen's behaviour under torsional loading. The numerical approach is validated against experimental data to ensure its accuracy and reliability. Furthermore, the paper presents an evaluation of the specimen's fatigue life based on the data collected, offering insights into the potential improvements this new setup could bring to fatigue testing methodology.

2. THEORETICAL BACKGROUND

2.1. Random Vibrations

It is customary to describe a random process, using a frequency function $S(\omega_i)$ called Power Spectral Density (PSD), where ω_i is the frequency. This function is characterized by the spectrals moments m_i as [6]:

$$m_i = \int_0^{+\infty} \omega^i S(\omega) d\omega \qquad i = 0 \text{ to } 4 \tag{1}$$

The combination of spectral moments is used to define the properties of the signal [6], such as the expectation of a positive zero crossing rate, ν_0 and the expectation of a peak rate ν_p:

$$\nu_0 = \sqrt{\frac{m_2}{m_0}} \qquad \nu_p = \sqrt{\frac{m_4}{m_2}} \tag{2}$$

2.2. Structural dynamic and modal analysis

The dynamic motion of a real structures can be described by the following expression [7]:

$$[M]\ddot{x} + [C]\dot{x} + [K]x = 0 \tag{3}$$

where $[M]$, $[C]$, and $[K]$ are respectively the mass matrix, the damping matrix and the stiffness matrix, $\boldsymbol{x}$ is the vector of displacements, and $\boldsymbol{f}$ is the excitation vector.

For a structure subjected to a base excitation, the absolute acceleration is computed as:

$$\ddot{\boldsymbol{x}}(t) = \ddot{\boldsymbol{y}}(t) + \ddot{\boldsymbol{z}}(t) \tag{4}$$

where $\ddot{\boldsymbol{y}}(t)$ and $\ddot{\boldsymbol{z}}(t)$ are the vectors of relative acceleration and base acceleration, respectively.

A steady state response to the base excitation can be rearranged as:

$$\boldsymbol{Y}(\omega) = \boldsymbol{H_{aa}}(\omega)[M]\ddot{\boldsymbol{Z}}(\omega) \tag{5}$$

where $\boldsymbol{H_{aa}}$ is the receptance matrix of the system which relates the kinematic base excitation to the relative structure acceleration responses [8].

For the purpose of a fatigue analysis under random loadings, stress components are described in the frequency domain by a following PSD-stress (MPa^2·Hz^{-1}):

$$\boldsymbol{S_s}(\omega) = \boldsymbol{H_s}(\omega)^T \boldsymbol{S_{in}}(\omega) \boldsymbol{H_s}(\omega) \tag{6}$$

where $\boldsymbol{H_s}(\omega)$ is defined as stress Frequency Response Function (MPa ·g^{-1})^2 and can be written as reported in [9], and $\boldsymbol{S_{in}}(\omega)$ is the input PSD-acceleration (g^2·Hz^{-1}).

2.3. Multi-axial criteria

The common way to assess the fatigue damage in a multi-axial stress is to reduce the stress component into an equivalent PSD-stress, indicated as $S_{eq}(\omega)$. In this paper two criteria are considered: the maximum normal stress [10] and the Preumont and Piefort criteria [11].

2.3.1. Preumont and Piefort criterion

Preumont and Piefort reformulated a new equivalent von Mises stress (EVMS) in frequency-domain [11]:

$$S_{eq}(\omega) = \int_0^\infty Tr\{\boldsymbol{Q}\boldsymbol{S_s}(\omega)\}d\omega \tag{7}$$

where $Tr\{\}$ is the trace function and $\boldsymbol{Q}$ is the following 6×6 matrix:

$$\boldsymbol{Q} = \begin{pmatrix} 1 & -1/2 & -1/2 & 0 & 0 & 0 \\ -1/2 & 1 & -1/2 & 0 & 0 & 0 \\ -1/2 & -1/2 & 1 & 0 & 0 & 0 \\ 0 & 0 & 0 & 3 & 0 & 0 \\ 0 & 0 & 0 & 0 & 3 & 0 \\ 0 & 0 & 0 & 0 & 0 & 3 \end{pmatrix} \tag{8}$$

2.4. Fatigue life assessment

Once the equivalent PSD-stress $S_{eq}(\omega)$ is calculated, it is possible to treat the equivalent signal with the uni-axial random approach, and the expected fatigue damage per unit time $E[D]$, may be evaluated by employing the following linear cumulative damage rule:

$$E[\overline{D}] = \nu_p C^{-1} \int_0^\infty s^b p(s) ds \tag{9}$$

where C and b are the parameters of the normal stress SN curve, s is the stress amplitude and $p(s)$ is the marginal amplitude distribution of the counted equivalent stress cycles, which, in the case of a narrow-band random, coincides with the Rayleigh distribution [6], and, consequently, Eq.(9) becomes:

$$E(D^{NB}) = \nu_p C^{-1} \left(\sqrt{2m_0}\right)^k \Gamma(1 + \frac{k}{2}) \tag{10}$$

where Γ denotes the Euler gamma function, defined as:

$$\Gamma(z) = \int_0^{(\infty)} t^{z-1} e^{-t} dt. \tag{11}$$

The calculated fatigue life T_{cal} is obtained as:

$$T_{cal} = \frac{1}{E[\overline{D}]} \tag{12}$$

3. LAYOUT OF TESTING SET-UP

Testing setup (Fig 1) is composed of a specimen, made of Complex Phase 800 steel, with two notches [12], glued to the top of an electromagnetic shaker. A T-mass shaped is mounted at the tip of the specimen to induce a contribution of bending-torsion stress.

Table 1: Mechanical properties of the testing set-up components.

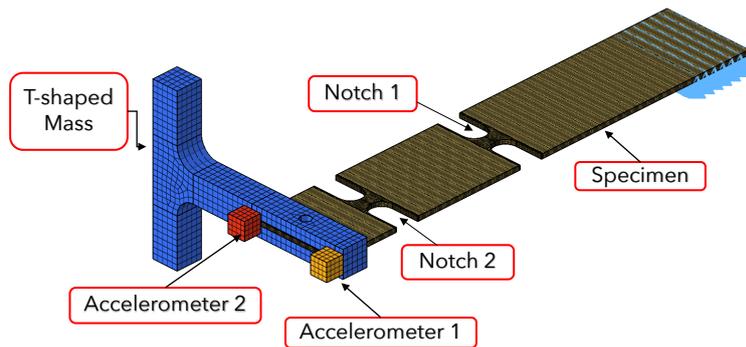| Component	Material	E [GPa]	Density [kg·m^{-3}]
Specimen	Steel	180	7740
T-mass shaped	Aluminum	72	2715

Figure 1: Numerical model of the testing set-up.

4. NUMERICAL ANALYSIS

Through numerical analysis, a suitable T-mass shaped dimension is defined for a fatigue life assessment. In addiction, an estimation of the dynamic performance and stress components in relation to different T-mass shaped dimensions, in analytical form, is executed.

4.1. T-mass shaped design phase

Three configurations were conceived, defining four geometric dimensions (a, b, c, and h as shown in Figure 2). During the design phase, dimensions b and c were increased by 50% and 75% over the initial setup (Table 2), with the mass component kept constant at 106.9 g. Resonant frequencies and natural modes were identified. The first mode is a bending mode, the second is a torsion alternating bending mode, the third is a bending mode, and the fourth is a pulsating bending mode. Analyzing the participation factors for each set-up (Table 3), the factor decreases for mode 1, increases for mode 2, and remains constant for mode 4. Mode 3, however, has a participation factor four orders of magnitude lower than the others and will be disregarded.
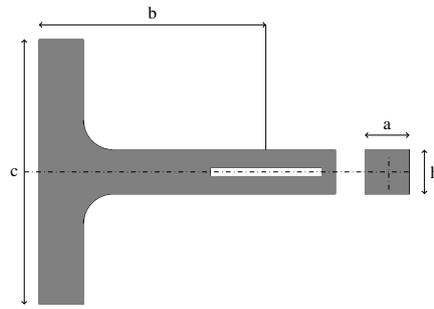
Figure 2: T-mass shaped profile.

Table 2: Dimensions of the three T-mass shaped geometrical configurations.

Configuration	a [mm]	b [mm]	c [mm]	h [mm]	Mass [g]
1	14.9	86.7	90.0	15.0	106.9
2	11.0	130.00	135.0	12.7	106.9
3	9.5	151.73	157.5	12.0	106.9

Table 3: Modal participation factors for each configuration.

Configuration	Mode 1	Mode 2	Mode 3	Mode 4
1	4.36E-01	8.69E-02	8.82E-06	1.89E-01
2	4.16E-01	1.39E-01	5.91E-05	1.90E-01
3	3.40E-01	1.62E-01	2.14E-05	1.93E-01

For all configurations, a constant acceleration frequency sweep 0.1g is applied and the maximal von Mises stress is evaluated. Based on the above consideration, only modes 2 and 4 are considered (Table 4). Both modes show an increase in stress. Mode 2 is the one that increases the most, while mode 4 turns out to be the one with the highest stress in all configurations.

Table 4: Maximum von Mises stress (in MPa) for each configuration.

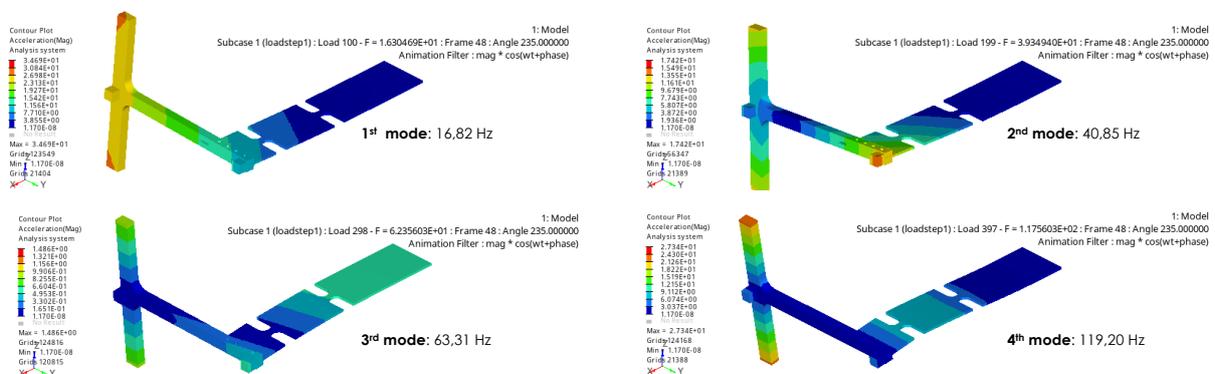| Configuration	Mode 2 [MPa]	± %	Mode 4 [MPa]	± %
1	2.98		34	
2	6.24	109	43.20	27
3	7.85	163	48.41	42

Figure 3: The first four mode shapes for the third configuration.

4.2. Linear Regression

An analytical relationship between input geometry parameters and stress components of the specimen offers insight into how the dynamic and stress behaviour of the specimen evolve with the changes of the T-mass dimensions. The input parameters are the ratio a/h, b/c and b. Three dimensions to each variable are assigned as reported in Tables 5.

Table 5: Values of the input variables.

Dimension	Variable		
	a/h	b/c	b
			[mm]
Low	0.8	0.75	86.7
Medium	1	0.96	130.05
High	1.2	1.25	151.725

Sixteen combinations of variables are defined. For each combination, the resonant frequencies for mode 1, mode 2 and mode 4, the maximal von Mises values for mode 2 and 4, and the stress components σ_{xx} and τ_{xy} for mode 2 are considered. The analytical model is created using a quadratic regression. Figure 4 presents the predicted values from the analytical model compared to the numerical data. The black line indicates an ideal correlation, and proximity to this line means stronger agreement. In terms of frequency resonance, all data points fell within an error margin of 2%. For stress components, some points showed errors greater than 2% yet stayed below 5% compared to numerical simulations, indicating a strong correlation between analytical and numerical models.

5. EXPERIMENTAL TESTS

First, the frequency response function of the experimental specimens are measured over the 30–150 Hz range under a constant base acceleration of 0.1 g. The numerical model is then updated according to the experiment, which allows a correct fit on the first four modes. Secondly, the FRF permits to obtain the eigenfrequencies of the modes that will be excited during the fatigue test.

The fatigue tests are then run by exciting the second and fourth modes with a band limited white noise PSD, according to the numerical study. Each PSD has a frequency range of 20 Hz and it is centred on the resonance frequency of the corresponding mode. The test is stopped either by the failing of the specimen or after 8 h, duration for which the specimen is considered to have survived. The comparisons between the average of experimental data for each PSD level and numerical results evaluations are illustrated in Fig.5 where the solid line indicates $T_{cal} = T_{exp}$, the dashed lines correspond to T_{cal}/T_{exp} equal to 0.5 and 2 , and the dash-dot lines correspond to T_{cal}/T_{exp} equal to 0.3 and 3.

Based on the results, the comparison seems to be quite satisfactory, with all the numerical results are included into the scatter band with coefficient 2 or 0.5. In the fourth mode, a better correlation is presented, with numerical results very close to the average value of experimental time to failure for all the PSD load level. In the second mode, the correlation seems less robust, firstly because failure times vary widely, especially for PSD level of 1.2 $g^2 \cdot Hz^{-1}$.

6. CONCLUSION

This study introduces a novel testing set-up for the assessment of multiaxial random vibrations and fatigue. Using both numerical and experimental methodologies, the research evaluates stress components, modal participation factors, and resonant frequencies in different configurations. Adaptations in the dimensions of the T-mass shaped influence the stress distribution and modal behaviour. The dynamic
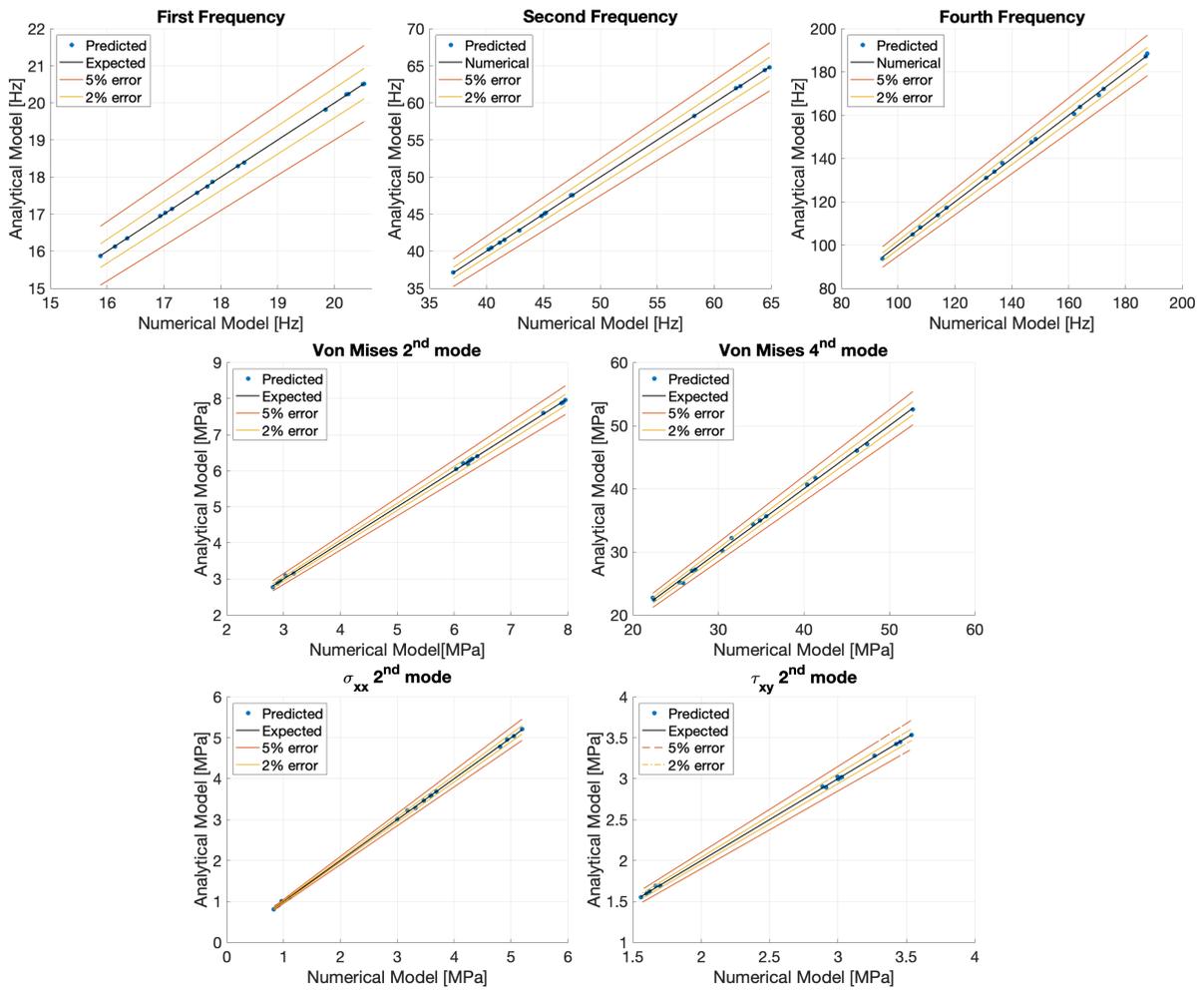
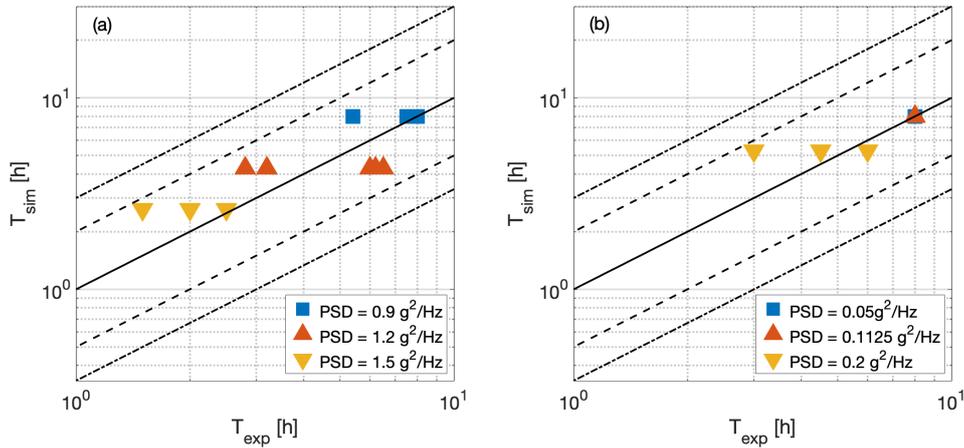**Figure 4:** Predicted value from analytical model compared to numerical results.

Figure 5: Testing results for mode 2 (a) and mode 4 (b).

model was validated through experimental tests. Later, the application of random vibrations assessed fatigue life. The results revealed different failure times for modes 2 and 4 at various Power Spectral Density levels, because of different state of stress conditions. Subsequently, the experimental outcomes are contrasted with established numerical techniques. It is found that the narrow band model accurately predicts the full bending mode, though it exhibits some inaccuracies in the torsion-bending mode. Further researches will enable authors to develop a new numerical model for damage identification when

subjected to a combined torsion-bending-torsion load

REFERENCES

[1] Ed Habtour, William Connon, Michael Pohland, Samuel Stanton, Mark Paulus, and Abhijit Dasgupta. Review of response and damage of linear and nonlinear systems under multiaxial vibration. *Shock and Vibration*, 2014, 2014.

[2] Wayne Whiteman and Morris Berman. Fatigue failure results for multi-axial versus uniaxial stress screen vibration testing. *Shock and Vibration*, 9:319–328, 2002.

[3] E. J. Marques, D. Benasciutti, A. Niesłony, and J. Slavič. An overview of fatigue testing systems for metals under uniaxial and multiaxial random loadings. *Metals*, 11, 2021.

[4] H. Rognon. Comportement en fatigue sous environnement vibratoire: prise en compe de la plasticite au sein des methodes spectrales, 2013.

[5] L. Campello, R. Sesana, R. Serra, and C. Delprete. Definition of an uni-axial equivalent testing procedure for a multi-axial random fatigue loading assessment. In *16ème Colloque National en Calcul des Structures*, 2024.

[6] J.S. Bendat and A.G. Piersol. *Random Data: Analysis and Measurement Procedures*. Wiley, 2011.

[7] L. Lutes and S. Sarkani. *Random Vibrations: Analysis of Structural and Mechanical Systems*. Elsevier, 2004.

[8] M. Česnik, J. Slavič, P. Čermelj, and M. Boltežar. Frequency-based structural modification for the case of base excitation. *Journal of Sound and Vibration*, 332(20):5029–5039, 2013.

[9] M. Mršnik, J. Slavič, and M. Boltežar. Vibration fatigue using modal decomposition. *Mechanical Systems and Signal Processing*, 98:548–556, 2018.

[10] Adam Niesłony and Ewald Macha. Spectral method in multiaxial random fatigue. *Zeszyty Naukowe. Mechanika/Politechnika Opolska*, (84):113–134, 2005.

[11] X. Pitoiset and A. Preumont. Spectral methods for multiaxial random fatigue analysis of metallic structures. *International Journal of Fatigue*, 22(7):541–550, 2000.

[12] V.K. Nagulapalli, A. Gupta, and S. Fan. Estimation of fatigue life of aluminum beams subjected to random vibration. *Conference Proceedings of the Society for Experimental Mechanics Series*, 01 2007.